JAIST Repository
https://dspace.jaist.ac.jp/

Title	Crystallographic and morphological characterization of thin pentacene films on polycrystalline copper surfaces
Author(s)	Oehzelt, M.; Resel, R.; Suess, C.; Friedlein, R.; Salaneck, W. R.
Citation	Journal of Chemical Physics, 124(5): 054711-1-054711-6
Issue Date	2006-02-03
Type	Journal Article
Text version	publisher
URL	http://hdl.handle.net/10119/4519
Rights	Copyright 2006 American Institute of Physics. This article may be downloaded for personal use only. Any other use requires prior permission of the author and the American Institute of Physics. The following article appeared in M. Oehzelt, R. Resel, C. Suess, R. Friedlein, W. R. Salaneck, Journal of Chemical Physics, 124(5), 054711 (2006) and may be found at http://link.aip.org/link/?JCPSA6/124/054711/1
Description	

JAIST
JAPAN
ADVANCED INSTITUTE OF
SCIENCE AND TECHNOLOGY

Japan Advanced Institute of Science and Technology

Crystallographic and morphological characterization of thin pentacene films on polycrystalline copper surfaces

M. Oehzelt[a] and R. Resel
Institute of Solid State Physics, Graz University of Technology, Petersgasse 16, A-8010 Graz, Austria

C. Suess, R. Friedlein, and W. R. Salaneck
Department of Physics (IFM), Linköping University, S-581 83 Linköping, Sweden

(Received 3 August 2005; accepted 18 November 2005; published online 3 February 2006)

The degree of crystallinity, the structure and orientation of crystallites, and the morphology of thin pentacene films grown by vapor deposition in an ultrahigh vacuum environment on polycrystalline copper substrates have been investigated by x-ray diffraction and tapping-mode scanning force microscopy (TM-SFM). Depending on the substrate temperature during deposition, very different results are obtained: While at 77 K a long-range order is missing, the films become crystalline at elevated temperatures. From a high-resolution x-ray-diffraction profile analysis, the volume-weighted size of the crystallites perpendicular to the film surface could be determined. This size of the crystallites increases strongly upon changing temperature between room temperature and 333 K, at which point the size of individual crystallites typically exceeds 100 nm. In this temperature region, three different polymorphs are identified. The vast majority of crystallites have a fiber texture with the (001) net planes parallel to the substrate. In this geometry, the molecules are oriented standing up on the substrate (*end-on* arrangement). This alignment is remarkably different from that on single-crystalline metal surfaces, indicating that the growth is not epitaxial. Additionally, TM-SFM images show needlelike structures which suggest the presence of at least one additional orientation of crystallites (*flat-on* or *edge-on*). These results indicate that properties of thin crystalline pentacene films prepared on technologically relevant polycrystalline metal substrates for fast electronic applications may be compromised by the simultaneous presence of different local molecular aggregation states at all temperatures. © *2006 American Institute of Physics*.
[DOI: 10.1063/1.2150826]

I. INTRODUCTION

While oligoacenes have been studied for more than a century,[1] interest in their use as crystalline or polycrystalline electronic materials has recently been boosted by the observation of high charge-carrier mobilities.[2] In the last few years, pentacene was successfully used as the active medium in organic field-effect transistors (OFETs),[3–7] Schottky diodes,[8–10] and photodiodes.[11–18] Oligoacenes are even interesting as a dye in organic solar cells.[19]

The large-scale integration of organic semiconductors into electronic devices often requires the use of technically relevant, polycrystalline metallic substrates. OFET devices using polycrystalline copper electrodes have been fabricated that perform as well as devices with gold contacts.[20] The interface between the molecules and polycrystalline copper substrates, especially as it affects the quality of the thin organic films, is in the focus of the present paper.

The crystal structures of bulk and thin films of pentacene (see Fig. 1) are still under discussion. Many polymorphs have been observed:[21,22] the single-crystal phase, denoted as **s**,[23,24] a so-called vapor-deposition phase, denoted as **v**,[25–29] and an additional thin-film phase, denoted as **t**.[30–34] With x-ray-diffraction techniques, the three different polymorphs can be distinguished by their (001) net plane spacings. The plane spacing d is 14.5 Å for **s**, 14.1 Å for **v**, and 15.4 Å for **t**. Several phase transitions have been reported: one between **s** and **v** under high pressure[35] and another one between **t** and **s** induced by a solvent.[22] In vapor-deposited thin films, **s** and **t** usually coexist.[36–44] It is important to understand for which film thicknesses and under which conditions the single-crystal phase **s** occurs and when the three polymorphs might coexist.

II. EXPERIMENT

The films were prepared in ultrahigh vacuum (UHV, base pressure of 1×10^{-10} mbar).[45] About 150-nm-thick copper films on oxidized Si(100) wafers were cleaned by Ne^+-ion etching followed by annealing at about 550 K in UHV. After cleaning, no traces of carbon and only a small amount of oxygen were detected by x-ray photoelectron spectroscopy (XPS). The organic molecules were then deposited from a resistably heated crucible (at constant temperature) onto the copper substrates, held at temperatures of either 77, 273, 293, 303, 313, 323, or 333 K. The deposition rate was less than 1 nm/min. The deposition of pentacene on copper substrates at temperatures higher than 333 K is not possible in vacuum, since the molecules do not adsorb on the substrate surface at these temperatures.

[a]Electronic mail: martin.oehzelt@tugraz.at

 © 2006 American Institute of Physics

Downloaded 10 Jun 2008 to 150.65.7.70. Redistribution subject to AIP license or copyright; see http://jcp.aip.org/jcp/copyright.jsp

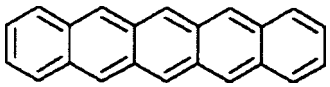

FIG. 1. Chemical structure of pentacene.

Following preparation, the samples were transferred in air to x-ray diffractometers and to the tapping-mode scanning force microscope and were characterized *ex situ* under ambient conditions. Various x-ray-diffraction methods have been applied, providing complementary information. $\theta/2\theta$ measurements were used to determine the crystallographic phases in the samples. The data were obtained from a Siemens D501 diffractometer in Bragg-Brentano geometry using Cu $K\alpha$ radiation monochromatized with a secondary graphite monochromator. With this technique, only net planes parallel to the surface of the substrate can be observed. The resolution was sufficient to allow a line-profile analysis for the determination of the volume-weighted size of the crystallites and of the strain within the organic layer. The instrumental parameters were determined using the line-profile standard LaB_6 NIST SRM 660a. In order to determine the relative orientation of crystallites with respect to the substrate surface, the x-ray-diffraction pole-figure method was employed.[46–52] The measurements were performed in Schultz reflection geometry[53] in a Philips X'Pert system with an ATC3 texture cradle using Cr $K\alpha$ radiation and a secondary graphite monochromator. For the x-ray-diffraction (XRD) data evaluation, the software packages POWDER CELL 2.3 (Ref. 54) and STEREOPOLE (Ref. 55) were used.

Complementary to the x-ray-diffraction measurements, tapping-mode scanning force microscopy (TM-SFM) was performed to obtain information about the morphology of the organic layers. Details of the measurements in a Nanoscope IIIa system (Digital Instruments, Santa Barbara, CA) are given elsewhere.[56]

III. RESULTS AND DISCUSSION

In Fig. 2, the x-ray pattern of the $\theta/2\theta$ scans for pentacene films prepared at 77, 293, 323, and 333 K is shown. The absence of diffraction peaks for the 77 K film indicates the missing of detectable long-range order. On the other hand, elevated temperatures during the film growth induce order. At 293 K, mainly the thin-film phase **t** grows on the substrate. Beginning with 323 K, also a small amount of the single-crystal phase **s** is detected. At a transition temperature of about 330 K, just a few degrees below the temperature where multilayer films could not be made anymore under vacuum conditions, the crystal growth mode changes again considerably. The main polymorphs at this deposition temperature are the two single-crystal structures. Figure 3 illustrates this dramatic change in the structural composition of the films. At higher angles of the $\theta/2\theta$ scans (not shown), copper peaks were also detected. With the Scherrer method[57] the crystallite size of the copper substrate could be determined to be approximately 10 nm for all the samples.

This transition and the coexistence of the single-crystal phase and the thin-film phase have already been reported for growth on passivated (oxidized) surfaces of SiO_2

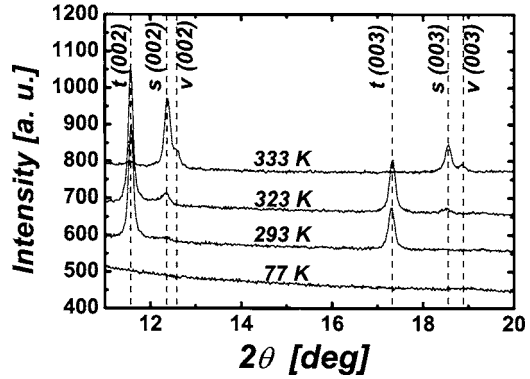

FIG. 2. $\theta/2\theta$ scans of thin pentacene films deposited at substrate temperatures of 77, 293, 323, and 333 K onto polycrystalline Cu substrates, indicating the evolution of three different polymorphs with the substrate temperature during deposition of pentacene. The abbreviation of the peaks **t**, **s**, and **v** denote the thin-film, the single-crystal, and the vapor-deposition phases, respectively.

(Refs. 36–42) and for Al_2O_3 (Ref. 43) as well as for Corning glass.[44] To the knowledge of the authors a coexistence of three of the polymorphs of pentacene has not been reported until now. To distinguish between the various phases, high-resolution measurements are required, especially since the vapor-deposition and single-crystal phases have a very similar $d(001)$ spacing. In Fig. 2, the two bulk phases are clearly distinguished in the x-ray pattern for the 333-K film. This pattern also indicates that the crystallites for these three pentacene polymorphs have predominantly a (001) orientation. That is, the molecules are standing on the substrate surface with the long molecular axes perpendicular to the surface (*end-on* alignment).

In the Bragg-Brentano geometry, reflections of net planes parallel to the surface of the substrate are detected. The line-profile analysis of these high-resolution patterns reveals information on the crystallite size and the strain in the direction perpendicular to the substrate surface. The accuracy of the line-profile analysis depends crucially on the separation of the instrumental broadening from the intrinsic linewidth generated by the sample itself. For an analytical expression of the broadening of the instrument, the model of Caglioti *et al.*[58] was adopted using the LaB_6 standard. In order to separate the two remaining intrinsic contributions, due to strain and the size of the crystallites, from each other, a Williamson-Hall analysis[59] is applied:

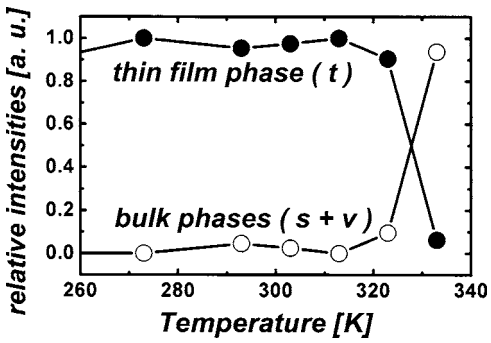

FIG. 3. Evolution of the relative intensities of the thin-film phase (○) with respect to the two bulk phases (●) as a function of the substrate temperature during the deposition of the organic material.

Downloaded 10 Jun 2008 to 150.65.7.70. Redistribution subject to AIP license or copyright; see http://jcp.aip.org/jcp/copyright.jsp

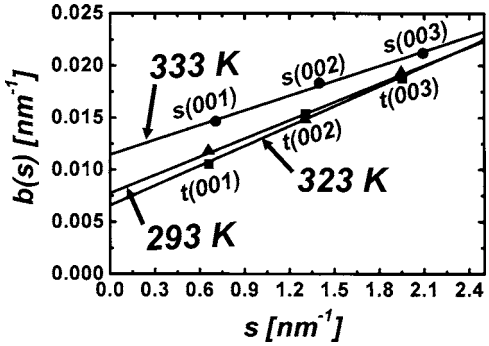

FIG. 4. Williamson-Hall plot of pentacene films deposited at 293, 323, and 333 K. The lines connecting the peak series are linear least-squares fits. The inverse of the ordinate interception equals the volume-weighted size of the crystallites in the film. The slope represents the root-mean-square strain.

$$b(s) = 1/\langle l\rangle_V + \sqrt{2\pi\langle\epsilon^2\rangle}\cdot s. \quad (1)$$

Here, s is the length of the scattering vector, $b(s)$ is the integral width of the peak, and $\langle l\rangle_V$ is the volume-weighted column length which is in this case the volume-weighted crystal size perpendicular to the surface. $\langle\epsilon^2\rangle$ is the mean-square (local) strain, whereas the whole root expression is the root-mean-square strain (*rms strain*).

The scattered intensity for the (001) net planes and its higher-order (002) and (003) reflections from the $\theta/2\theta$ scans depicted in Fig. 2 were high enough to allow a peak profile analysis. Pseudo-Voight-shaped profile functions were used to fit the individual peaks.[60,61] The Williamson-Hall plots are depicted in Fig. 4. For each sample the three points are on line which reveal the desired parameters: $1/\langle l\rangle_V = (0.0077\pm0.0009)$ cm^{-1} and rms strain$=(0.0059\pm0.0006)$ for the 293 K sample, $1/\langle l\rangle_V=(0.0066\pm0.0009)$ cm^{-1} and rms strain$=(0.0064\pm0.0007)$ for the 323 K sample, as well as $1/\langle l\rangle_V=(0.0115\pm0.0005)$ cm^{-1} and rms strain $=(0.0047\pm0.0003)$ for the 333 K sample. From this fit parameters, the volume-weighted size of the crystallites perpendicular to the substrate surface amounts to (129 ± 15) nm for the 293 K sample, (150 ± 20) nm for the 323 K sample, and (87 ± 4) nm for the 333 K sample.

In addition to the symmetric $\theta/2\theta$ measurements, x-ray pattern in pole-figure geometry were recorded. In this geometry, net planes that are inclined with respect to the substrate can also be observed. The distribution of a single net plane specified by the 2θ value of the sample is recorded and results in the determination of the spherical distribution of that net plane. As the index of the net plane parallel to the substrate surface is already known from the $\theta/2\theta$ scans, the appropriate distribution of the azimuthal crystallite orientation is uniquely determined[46,48] and represented in the pole figures. Figure 5 shows two of these patterns: the upper one is recorded for the (002) plane of copper, while the lower pattern shows the distribution of planes with the net plane distance of 4.5 Å for the pentacene film deposited at 333 K. For this distance, the net planes from the single-crystal structure **s**, (110), and from the vapor-deposition structure **v**, (112), generate intensities. Both planes are easily distinguished as they appear at different angles with respect to the (001) plane visible by the different ring radii in the pole figure. A rather homogeneous distribution of pole densities along the rings implies that while the specific net plane is essentially parallel to the substrate surface, the azimuthal angle of this plane is equally distributed. That is, the azimuthal orientation of the crystallites is random. This type of distribution of pole densities along the rings is called "fiber texture" (see Fig. 5).

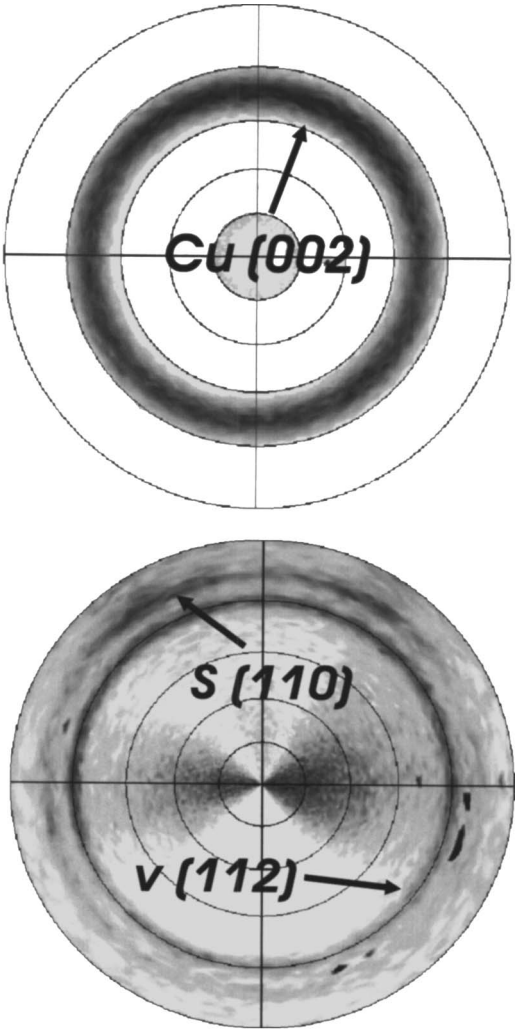

FIG. 5. Pole figure of the copper substrate (above) and the pentacene layer deposited at 333 K (below). Both show a fiber texture but the angular spread of the alignment of copper is much higher as it is for the pentacene layer and its polymorphs, as indicated by the width of the rings.

The radial pole density along a line through the center of the pole figure is a rocking curve. The peak width of the rocking curves (which means in this case the width of the recorded rings) is a measure of the spread and alignment of the crystallites with respect to the substrate. For the pentacene film made at 333 K, the width of the Cu pole densities (see Fig. 5, upper pole figure) is much larger than that of the individual pentacene rings. Crystallites of the copper substrate are therefore less aligned to each other than those of the organic layer.

The main result of this study is that major parts of the pentacene films grown at ambient substrate temperatures have a (001) orientation (end-on) independent of the specific

Downloaded 10 Jun 2008 to 150.65.7.70. Redistribution subject to AIP license or copyright; see http://jcp.aip.org/jcp/copyright.jsp

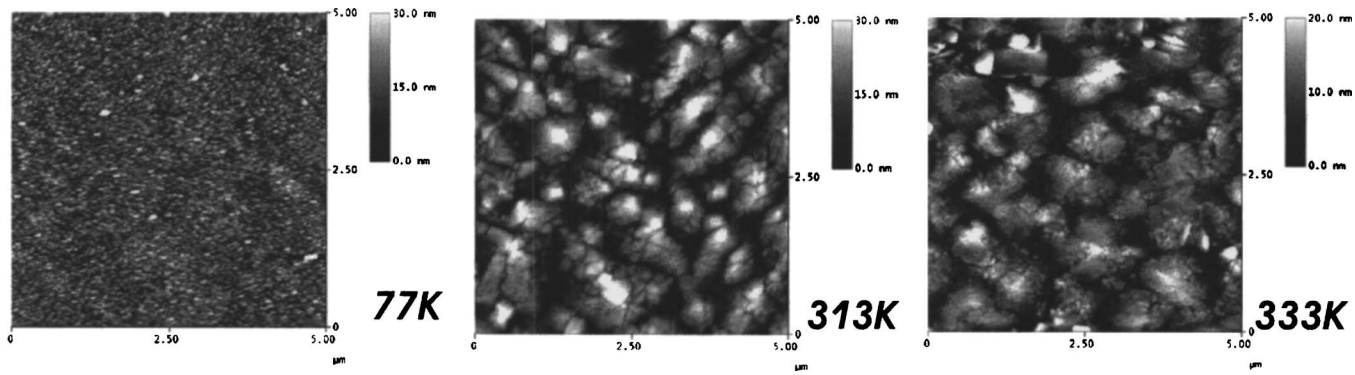

FIG. 6. The morphology of pentacene films deposited on polycrystalline copper substrates at different substrate temperatures. All TM-SFM images show 5×5 μm^2 sections of the surface. The gray scale ranges from 0 to 30 nm for the films prepared at 77 and 313 K. For the third image the scale ranges from 0 to 20 nm.

distribution of crystal phases. This particular orientation of the crystallites is remarkably different as on many metallic surfaces pentacene molecules are lying (*flat-on*),[62,63] leading to a clearly different alignment of the net planes.[64–68] A flat-on or edge-on arrangement is observed for a number of organic molecules on single-crystal surfaces. For example, the rodlike molecule quaterphenyl (with an isomorph crystal structure) prefers to lie when deposited on the Au(110) substrates.[69,70] Other examples are large discotic polyaromatic molecules, such as copper phthalocyanine and hexa-peri-hexabenzocoronenes, which in films of a thickness similar to that in our films are oriented flat-on on the Au(110) and MoS_2(0001) single-crystal surfaces, respectively.[56,71] Note that on the technically relevant polycrystalline substrates, the orientation of both copper phthalocyanine[71] and pentacene molecules is radically different from that in films grown on single crystals.

In the present pentacene/polycrystalline Cu system, the domains in the substrate are typically smaller than 10 nm, not much larger than the length of the molecules of about 1.5 nm. Since the molecular orientation is different to that on single-crystal substrates and since the lateral size of pentacene crystallites is far larger than that of the domains in the underlying substrate, it is obvious that the formation of pentacene crystallites is not driven by the interaction with the substrate. It appears that the substrate domains are too small to form a template suitable to initiate epitaxial growth. These considerations might explain why the pentacene crystallites grow end-on.

TM-SFM images of layers grown at different temperatures are presented in Fig. 6. The film grown at 77 K shows very small grains. Since the x-ray pattern is featureless, a long-range order in these grains is missing. At elevated temperatures, the grains become larger and a terracelike morphology develops which is consistent with an end-on arrangement of the molecules. The transition from the thin-film phase to the bulk phases does not change the morphology of the films.

Additionally to the terracelike morphology needles have been observed in films prepared at various substrate temperatures. Figure 7 shows such a structure for a 303-K film. Needlelike structures sometimes result from molecules lying at the substrate.[51,52] For such an orientation, Bragg reflections other than those of the (001) series have to be present in the x-ray pattern. And indeed, a peak at around 24.1° in the $\theta/2\theta$ scan of the film deposited at 323 K (Fig. 8) cannot be explained in terms of the (001) orientations of the net planes parallel to the substrate surface. This position matches the (022) peak of the polymorph **v**.[44] The same peak is present for films made on Corning glass,[44] but it is not

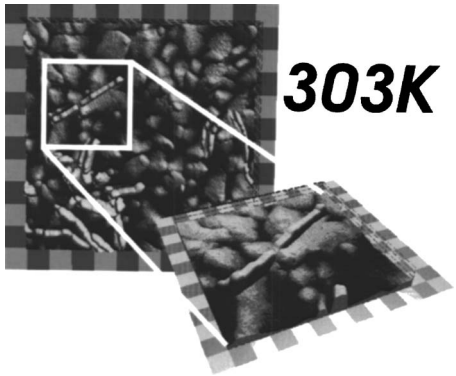

FIG. 7. TM-SFM image of a pentacene film deposited at a substrate temperature of 303 K showing a needlelike structure. The overview shows a 5×5 μm^2 region of the sample. The three-dimensional image is a close-up region of 2×2 μm^2 displaying details of the needle morphology.

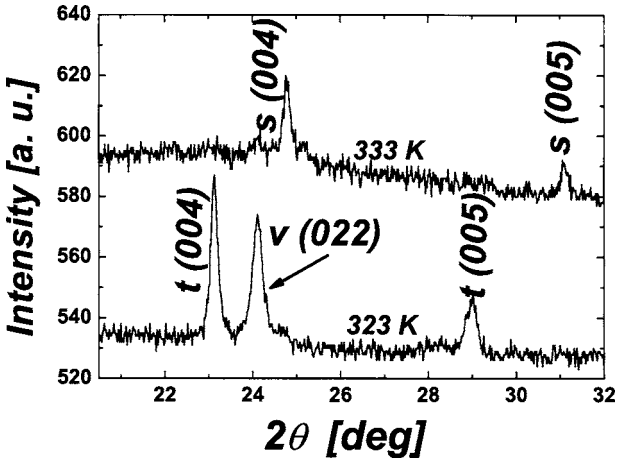

FIG. 8. $\theta/2\theta$ scans of pentacene thin films deposited at substrate temperatures of 323 and 333 K. The scan of the film deposited at 323 K shows clearly an additional orientation to the (001) orientation.

Downloaded 10 Jun 2008 to 150.65.7.70. Redistribution subject to AIP license or copyright; see http://jcp.aip.org/jcp/copyright.jsp

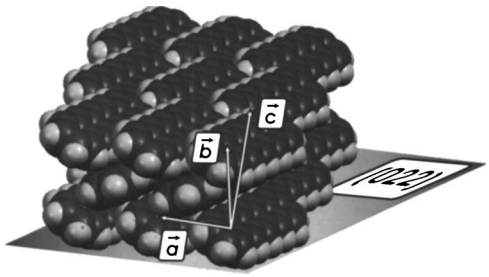

FIG. 9. Schematic drawing of the pentacene net plane (022) of the vapor-deposition phase **v**.

indexed. The (022) plane is also a cleavage plane (Fig. 9) and indicates that the growth of the needles occurs with this plane parallel to the substrate.

From the TM-SFM images in Fig. 6, the lateral dimensions of the grains can be estimated to be about 1 μm in diameter. However, it should be assumed that individual grains consist of more than one crystallite. As the substrate is not seen in the images, the height of the crystallites is not accessible by TM-SFM. This parameter can be determined by a line-profile analysis of the x-ray measurements shown in Fig. 4 followed by a size/strain analysis. The average height increases from about 129 nm at 293 K to about 150 nm at 323 K. In the transition region at about 333 K, where a mixture of all three polymorphs is present, the crystallite size is with about 87 nm considerably lower. The evaluation of the rms strain within the film rounds up the picture: 0.0059 at 293 K, 0.0064 at 323 K, and 0.0047 at 333 K. That is, strain is mainly constant near the transition point at 330 K and is released at higher temperature.

IV. CONCLUSION

The growth of thin pentacene films on technically relevant polycrystalline copper substrates has been studied as a function of the substrate temperature during the deposition of the organic film. While at low temperatures (77 K) a long-range order is missing, at ambient temperatures molecules are mobile enough to form a multitude of crystalline phases. In particular, three different polymorphs are observed where the composition of the films changes at a phase-transition temperature of about 330 K from the thin-film polymorph to the two single-crystal bulk structures. However, independent of the temperature, the large majority of crystallites align with the (001) net planes parallel to the substrate. Only a minor contributions are needlelike structures where the molecules have a flat-on arrangement with respect to the substrate surface.

The observed dominant end-on molecular alignment and therefore the orientation of crystallites are remarkably different from that in pentacene films grown on single-crystal copper surfaces. Evidence is found that the texture of the organic films does not follow the texture of the underlying polycrystalline copper substrate. This indicates that when the grains in the substrate are too small, the interaction between the molecules and the surface becomes too weak to allow epitaxial growth.

While the films made at ambient temperatures are overall remarkably crystalline, the simultaneous presence of several crystalline phases cannot be avoided when using polycrystalline copper substrates but is controlled by the choice of the deposition parameters and the substrate quality. Consequences for the transport of charge carriers and for the functioning of organic electronic devices based on pentacene may be severe and remain to be investigated in detail.

ACKNOWLEDGMENTS

This research project is supported by the Austrian Science Foundation (Project No. P15626-PHY) and the foreign affairs division of the Graz University of Technology. One of the authors (M.O.) also acknowledges support from the Austrian Research Society (ÖFG). The work performed in Linköping is supported by the Swedish Science Council (VR; Project No. 12252020), partially by the EU-Growth project MAC-MES (Project no. GRD2-2000-30242), and by the Center for Advanced Molecular Materials (CAMM) funded by SSF.

[1] A. Pochettino, Acad. Lincei Rend. 15, 355 (1906).
[2] N. Karl, *Organic Semiconductors*, Landolt-Börnstein, New Series, Group III, Vol. 17 (Springer-Verlag, Berlin, 1985).
[3] Y. Y. Lin, D. J. Gundlach, S. F. Nelson, and T. N. Jackson, IEEE Trans. Electron Devices **44**, 1325 (1997).
[4] Z.-T. Zhu, J. T. Mason, R. Dieckmann, and G. G. Malliaras, Appl. Phys. Lett. **81**, 4643 (2002).
[5] M. Halik, H. Klauk, U. Zschieschang, T. Kriem, G. Schmid, W. Radlik, and K. Wussow, Appl. Phys. Lett. **81**, 289 (2002).
[6] M. Kitamura, T. Imada, and Y. Arakawa, Appl. Phys. Lett. **83**, 3410 (2003).
[7] J. Zaumseil, T. Someya, Z. Bao, Y.-L. Loo, R. Cirelli, and J. A. Rogers, Appl. Phys. Lett. **82**, 793 (2003).
[8] Y. S. Lee, J. H. Park, and J. S. Choi, Opt. Mater. (Amsterdam, Neth.) **21**, 433 (2002).
[9] S. Kuniyoshi, S. Naruge, M. Iizuka, M. Nakamura, K. Kudo, and K. Tanaka, Synth. Met. **137**, 895 (2003).
[10] J. Lee, D. K. Hwang, C. H. Park, S. S. Kim, and S. Im, Thin Solid Films **451**, 12 (2004).
[11] G. Jarosz, R. Signerski, and J. Godlewski, Synth. Met. **109**, 161 (2000).
[12] G. Jarosz, R. Signerski, and J. Godlewski, Thin Solid Films **396**, 196 (2001).
[13] J. Godlewski, G. Jarosz, and R. Signerski, Appl. Surf. Sci. **175**, 344 (2001).
[14] R. Signerski, G. Jarosz, and J. Godlewski, Synth. Met. **94**, 135 (1998).
[15] Y. Vertsimakha and A. Verbitsky, Synth. Met. **109**, 291 (2000).
[16] J. Lee, S. S. Kim, K. Kim, J. H. Kim, and S. Im, Appl. Phys. Lett. **84**, 1701 (2004).
[17] S. S. Kim, Y. S. Choi, K. Kim, J. H. Kim, and S. Im, Appl. Phys. Lett. **82**, 639 (2002).
[18] S. P. Park, S. S. Kim, J. H. Kim, C. N. Whang, and S. Im, Appl. Phys. Lett. **80**, 2872 (2002).
[19] G. K. R. Senadeera, P. V. V. Jayaweera, V. P. S. Perera, and K. Tennakone, Sol. Energy Mater. Sol. Cells **73**, 103 (2002).
[20] D. J. Gundlach (private communication).
[21] R. G. D. Valle, E. Venuti, A. Brillante, A. Girlando, ChemPhysChem **5**, 266 (2004).
[22] D. J. Gundlach, T. N. Jackson, D. G. Schlom, and S. F. Nelson, Appl. Phys. Lett. **74**, 3302 (1999).
[23] R. B. Campbell, J. M. Robertson, and J. Trotter, Acta Crystallogr. **14**, 705 (1961).
[24] R. B. Campbell, J. M. Robertson, and J. Trotter, Acta Crystallogr. **15**, 289 (1962).
[25] D. Homes, S. Kumaraswamy, A. J. Matzger, and K. P. Vollhardt, Chem.-Eur. J. **5**, 3399 (1999).

Downloaded 10 Jun 2008 to 150.65.7.70. Redistribution subject to AIP license or copyright; see http://jcp.aip.org/jcp/copyright.jsp

[26] C. C. Mattheus, A. B. Dros, J. Baas, A. Meetsma, J. L. de Boer, and T. T. M. Palstra, Acta Crystallogr., Sect. C: Cryst. Struct. Commun. **57**, 939 (2001).
[27] C. C. Mattheus, A. B. Dros, J. Baas, G. T. Oostergetel, A. Meetsma, J. L. de Boer, and T. T. M. Palstra, Synth. Met. **138**, 475 (2002).
[28] C. C. Mattheus, G. A. de Wijs, R. A. de Groot, and T. T. M. Palstra, J. Am. Chem. Soc. **125**, 6323 (2003).
[29] G. A. de Wijs, C. C. Mattheus, R. A. de Groot, and T. T. M. Palstra, Synth. Met. **139**, 109 (2003).
[30] T. Minakata, H. Imai, M. Ozaki, and K. Saco, J. Appl. Phys. **72**, 5220 (1992).
[31] T. Minakata, H. Imai, and M. Ozaki, J. Appl. Phys. **72**, 4174 (1992).
[32] J. E. Northrup, M. L. Tiago, and S. G. Louie, Phys. Rev. B **66**, 121404 (2002).
[33] F.-J. zu Heringdorf, M. C. Reuter, and R. M. Tromp, Nature (London) **412**, 517 (2001).
[34] R. Ruiz, B. Nickel, N. Koch, L. C. Feldman, R. F. Haglund, A. Kahn, and G. Scoles, Phys. Rev. B **67**, 125406 (2003).
[35] L. Farina, A. Brillante, R. G. D. Valle, E. Venuti, M. Amboage, and K. Syassen, Chem. Phys. Lett. **375**, 490 (2003).
[36] C. D. Dimitrakopoulos, A. R. Brown, and A. Pomp, J. Appl. Phys. **80**, 2501 (1996).
[37] D. J. Gundlach, Y. Y. Lin, T. N. Jackson, S. F. Nelson, and D. G. Schlom, IEEE Electron Device Lett. **18**, 87 (1997).
[38] D. Knipp, R. A. Street, B. Krusor, R. Apte, and J. Ho, J. Non-Cryst. Solids **299**, 1042 (2002).
[39] D. Knipp, R. A. Street, A. Völkel, and J. Ho, J. Appl. Phys. **93**, 347 (2003).
[40] M. Shtein, J. Mapel, J. B. Benzinger, and S. R. Forrest, Appl. Phys. Lett. **81**, 268 (2002).
[41] T. Jentzsch, H. J. Juepner, K.-W. Brzezinka, and A. Lau, Thin Solid Films **315**, 273 (1998).
[42] I. P. M. Bouchoms, W. A. Schoonveld, J. Vrijmoeth, and T. M. Klapwijk, Synth. Met. **104**, 175 (1999).
[43] J. Lee, J. H. Kim, and S. Im, J. Appl. Phys. **95**, 3733 (2004).
[44] J. Puigdollers, C. Voz, A. Orpella, I. Martin, M. Vetter, and R. Alcubilla, Thin Solid Films **427**, 367 (2003).
[45] R. Friedlein, X. Crispin, M. Pickholz, M. Keil, S. Stafström, and W. R. Salaneck, Chem. Phys. Lett. **354**, 389 (2002).
[46] L. E. Alexander, *X-Ray Diffraction Methods in Polymer Science* (Robert E. Krieger, Huntington, New York, 1979).
[47] B. Servet, S. Ries, M. Trotel, P. Alont, G. Horowitz, and F. Garnier, Adv. Mater. (Weinheim, Ger.) **5**, 461 (1993).
[48] J. Kečkeš, B. Ortner, J. Jakabovič, and F. Kováč, J. Cryst. Growth **192**, 84 (1998).
[49] S. R. Forrest, Chem. Rev. (Washington, D.C.) **97**, 1030 (1997).
[50] S. R. Forrest, M. L. Kaplan, and P. H. Schmidt, J. Appl. Phys. **56**, 543 (1984).
[51] R. Resel, Thin Solid Films **433**, 1 (2003).
[52] H. Plank, R. Resel, S. Purger, J. Keckes, A. Tierry, B. Lotz, A. Andreev, N. S. Sariciftci, and H. Sitter, Phys. Rev. B **64**, 235423 (2001).
[53] L. G. Schultz, J. Appl. Phys. **20**, 1030 (1949).
[54] W. Kraus and G. Nolzeb, J. Appl. Crystallogr. **29**, 301 (1996).
[55] I. Salzmann and R. Resel, J. Appl. Crystallogr. **37**, 1029 (2004).
[56] R. Friedlein, X. Crispin, C. Simpson *et al.*, Phys. Rev. B **68**, 195414 (2003).
[57] B. E. Warren, *X-Ray Diffraction* (Addison-Wesley, Reading, MA, 1969).
[58] G. Caglioti, A. Paoletti, and R. Ricci, Nucl. Instrum. Methods 35, 223 (1958).
[59] G. Williamson and W. Hall, Acta Metall. **1**, 22 (1953).
[60] R. Snyder, J. Fiala, and H. Binge, *IUCr Monographs on Crystallography 10* (Oxford University Press, New York, 1999).
[61] R. Young, *IUCr Monographs on Crystallography 5* (Oxford University Press, New York, 1993).
[62] S. Lukas, S. Söhnchen, G. Witte, and C. Wöll, ChemPhysChem **5**, 266 (2004).
[63] S. Lukas, G. Witte, and C. Wöll, Phys. Rev. Lett. **88**, 028301 (2002).
[64] V. Corradini, C. Menozzi, M. Cavallini, F. Biscarini, M. G. Betti, and C. Mariani, Surf. Sci. **532**, 249 (2003).
[65] C. Menozzi, V. Corradini, M. Cavallini, F. Biscarini, M. G. Betti, and C. Mariani, Thin Solid Films **428**, 227 (2003).
[66] Y. L. Wang, W. Ji, D. X. Shi, S. X. Du, C. Seidel, Y. G. Ma, H.-J. Gao, L. F. Chi, and G. Fuchs, Phys. Rev. B **69**, 075408 (2004).
[67] J. H. Kang and X.-Y. Zhu, Appl. Phys. Lett. **82**, 3248 (2003).
[68] P. G. Schroeder, C. B. France, J. B. Park, and B. A. Parkinson, J. Appl. Phys. **91**, 3010 (2002).
[69] S. Müllegger, I. Salzmann, R. Resel, and A. Winkler, Appl. Phys. Lett. **83**, 4536 (2003).
[70] S. Müllegger, O. Stranik, E. Zojer, and A. Winkler, Appl. Surf. Sci. **221**, 184 (2004).
[71] H. Peisert, T. Schwieger, J. M. Auerhammer, M. Knupfer, M. S. Golden, J. Fink, P. R. Bressler, and M. Mast, J. Appl. Phys. **90**, 466 (2001).

Downloaded 10 Jun 2008 to 150.65.7.70. Redistribution subject to AIP license or copyright; see http://jcp.aip.org/jcp/copyright.jsp